Cross section and γ-ray spectra for ^{238}U(n,γ) measured with the DANCE detector array at the Los Alamos Neutron Science Center

J. L. Ullmann,[*] T. Kawano, T. A. Bredeweg, A. Couture, R. C. Haight, M. Jandel, J. M. O'Donnell, R. S. Rundberg,
D. J. Vieira, and J. B. Wilhelmy
Los Alamos National Laboratory, Los Alamos, New Mexico 87545, USA

J. A. Becker, A. Chyzh, and C. Y. Wu
Lawrence Livermore National Laboratory, Livermore, California 94550, USA

B. Baramsai and G. E. Mitchell
North Carolina State University, Raleigh, North Carolina 27607, USA

M. Krtička
Charles University, Prague, Czech Republic

Background: Accurate knowledge of the ^{238}U(n,γ) cross section is important for developing theoretical nuclear reaction models and for applications. However, capture cross sections are difficult to calculate accurately and often must be measured.

Purpose: We seek to confirm previous measurements and test cross-section calculations with an emphasis on the unresolved resonance region from 1 to 500 keV.

Method: Cross sections were measured from 10 eV to 500 keV using the DANCE detector array at the LANSCE spallation neutron source. The measurements used a thin target, 48 mg/cm^2 of depleted uranium. Gamma cascade spectra were also measured to provide an additional constraint on calculations. The data are compared to cross-section calculations using the code CoH$_3$ and cascade spectra calculations made using the code DICEBOX.

Results: This new cross-section measurement confirms the previous data. The measured gamma-ray spectra suggest the need for additional low-lying dipole strength in the radiative strength function. New Hauser-Feshbach calculations including this strength accurately predict the capture cross section without renormalization.

Conclusions: The present cross-section data confirm previous measurements. Including additional low-lying dipole strength in the radiative strength function may lead to more accurate cross-section calculations in nuclei where $\langle \Gamma_\gamma \rangle$ has not been measured.

PACS number(s): 25.40.Lw, 27.90.+b, 28.20.Np

I. INTRODUCTION

Accurate knowledge of the ^{238}U(n,γ) cross section from thermal energies to a few MeV is important for many applications, including calculations of the properties of nuclear power reactors. There have been many measurements made over the years that are documented in the EXFOR data library [1]. Early evaluations of the data tended to favor cross sections in the keV region that were in the upper range of measured values and were considered to be too high to be consistent with careful analysis of power reactor parameters. Subsequent reanalysis of the data and the use of new evaluation techniques resulted in lower cross sections that gave better agreement [2,3]. In a recent evaluation of nuclear data standards, Carlson *et al.* [4] did not include ^{238}U(n,γ) as a standard, but subjected the data to an evaluation of similar rigor, producing a new table of accepted values.

There have been few recent measurements of ^{238}U(n,γ) cross sections, and changes in the evaluated cross sections have been largely due to reanalysis of existing data, new methods for evaluation, or combining the results of different measurements. In this paper we will present the results of a new measurement of the ^{238}U(n,γ) cross section from 10 eV to 500 keV using the Detector for Advanced Neutron Capture Experiments (DANCE) at the Los Alamos Neutron Science Center, with particular emphasis on the unresolved resonance region above about 1 keV. By measuring the full energy of the capture gamma cascade, DANCE provides control of external backgrounds and backgrounds due to scattering of neutrons from the sample. The high efficiency of DANCE, combined with the high neutron flux at LANSCE, enabled the use of thinner targets that minimized the self-attenuation and multiple scatter corrections. The cross sections are normalized to well resolved weak resonances near 100 eV.

Calculations of the gamma-ray spectra and capture cross section were made. The gamma-ray spectra provide an additional constraint on the radiative strength function. Hauser-Feshbach calculations of the capture cross section from 1 to 500 keV, using a radiative strength function that provided a good representation of the gamma-ray spectrum, are in very good agreement with the measured values.

---

*[*]ullmann@lanl.gov

II. EXPERIMENT

A. Experiment setup

The DANCE array is located on Flight Path 14 at the Manuel J. Lujan, Jr. Neutron Scattering Center at the Los Alamos Neutron Science Center (LANSCE). Flight Path 14 views the upper-tier room-temperature water moderator. The sample location is 20.25 m from the moderator. Neutrons were tightly collimated to a 0.7 cm diameter beam spot with minimal penumbra at the sample location. DANCE consists of a spherical array of 160 BaF_2 crystals, each 734 cm^3 in volume with faces located 19 cm from the beam center. The array covers a total solid angle of approximately 3.5π steradians. The high photopeak efficiency of the BaF_2, coupled with the high segmentation of the array, make it ideal for measuring the multiplicity and total energy of the gamma-ray cascade following neutron capture.

The gamma-ray energy calibration was determined crystal by crystal using a variety of radioactive sources and checked periodically using an [88]Y source. Run-by-run drifts were monitored and corrected using the alpha decay peaks from nuclides in the [226]Ra decay chain which occurs naturally in the BaF_2 crystals. The alpha peaks can be separated from gamma rays using the pulse-shape discrimination properties of BaF_2. The relative timing of each crystal was determined from time coincidences in an event, and adjusted to give minimal dispersion. The total time dispersion between all crystals in an event was 2 ns FWHM. A time coincidence window of ± 10 ns was applied during data analysis.

The DANCE data acquisition system consists of two 8-bit transient digitizers per crystal. For this measurement, the digitizers had a 2 ns sampling interval, and were each set to cover a 250 μs range. Time-of-flight timing and pulse area were determined from the digitized signal. The trigger delay with respect to the beam pulse for each digitizer was variable. Most commonly the first digitizer delay was set to -10 μs and the second to 240 μs, covering a continuous neutron energy range down to 10 eV.

The neutron flux as a function of energy was determined by three neutron monitors located downstream of the sample location. The monitors used the [6]Li(n,αt) reaction, the [235]U($n,$f) reaction, and the [3]He($n,$p) reaction. In this measurement, the [3]He monitor was used only for a consistency check. The digitizers for the neutron monitors had a 50 ns sample interval and a 14 ms range to cover energies to below thermal. The flux in the 1 eV to 100 keV range, measured at the [6]Li monitor location, was roughly $(1.08 \times 10^4)/E^{-1.033}$ neutrons/(cm^2 eV s), where E is the neutron energy in eV, for a proton beam current of 100 μA. The measured neutron flux is shown in Fig. 1. In order to reduce the statistical uncertainty, the flux was averaged over 176 hours of beam with various thin backing foils (Be, Ti, kapton) in the target position. There is a strong resonance in the [6]Li($n,$t) cross section at about 239 keV which introduced complexities in the flux determination, so the [235]U($n,$f) reaction was used to determine the flux above 10 keV. A composite flux was obtained by normalizing the flux from [235]U($n,$f) to that from [6]Li($n,$t) over the region from 3 to 10 keV, and using the normalized flux determined from [235]U($n,$f) above 10 keV. The statistical uncertainty of the flux in 2% bins at
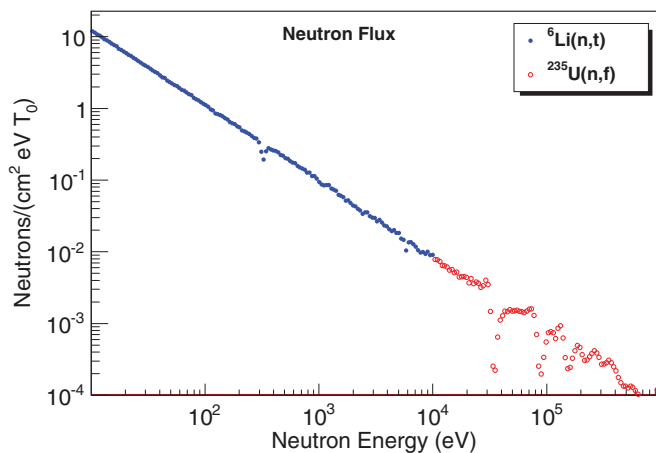

FIG. 1. (Color Online) Composite neutron flux at the [6]Li monitor location binned in $dE/E = 5\%$ bins. The flux measured with the [235]U($n,$f) reaction was normalized to the [6]Li as described in the text. The flux is normalized to neutrons per beam burst (T_0); there are 20 beam bursts per second. The proton beam current was 100 μA.

1 keV was 3.5%, and in 5% bins at 100 keV roughly 2%. The cross section, however, is normalized to known resonances as described in Sec. II C. The dips in the flux at 34.8, 86.2, and 142.3 keV are due to strong resonances in [27]Al that occurs in the moderator and beam windows. Reliable cross-section measurements could not be made at these resonance energies.

Neutrons scattered from the sample can be detected through capture on the barium in the array crystals, producing a gamma-ray background. A [6]LiH shell, fabricated from [6]Li enriched to 86%, with inner radius 10.5 cm and outer radius 16.5 cm surrounds the sample location to reduce the contribution from scattered neutrons, but it remains an important background component for neutron energies above a few keV.

The cross-section measurements were made with a 48 mg/cm^2 depleted uranium foil (approximately 99.8% [238]U). The gamma-ray spectrum measurements were made with a target consisting of 2.27 mg/cm^2 $\pm 4\%$ [238]U (99.98% enriched) deposited on a 2.5 μm Ti foil. Both targets were enclosed in a target holder with 76 μm Kapton windows. In addition, scatter background measurements were made with a 30.5 mg/cm^2 [208]Pb foil, enriched to 98.4%.

A single gamma ray interacting in DANCE can produce signals in several crystals because of pair production and Compton scattering. Signals in adjacent crystals are grouped together as a "cluster", and it has been shown that the energy and multiplicity (M_{cl}) of the cluster is proportional to the actual gamma-ray energy and multiplicity [5].

B. Background subtraction

Accurate and precise background subtraction is crucial to obtaining the neutron-capture cross section. There are two dominant classes of backgrounds in DANCE: low-energy positrons and gammas that can often be eliminated by cuts on the summed-energy spectrum, and backgrounds from neutron capture on the barium isotopes in the BaF_2 crystals. The low-energy positrons come from beta decay of nuclides in

the ^{226}Ra decay chain, in particular ^{214}Bi and ^{214}Pb with Q_β of 3.3 and 1.0 MeV, respectively. Ra occurs naturally in the BaF$_2$ crystals since it is a chemical homologue of Ba, and is present after the Ba chemical purification. This background can be precisely measured and subtracted if necessary. An additional source of low-energy background is due to gamma rays present in the neutron beam which can Compton scatter or pair-produce in the target. It is believed that the main source of these gamma-rays is from the $n + p \rightarrow d + \gamma$ reaction in the water moderator resulting in 2.2 MeV gamma rays, although other sources may also contribute.

The neutron backgrounds have two sources: ambient neutrons present when the shutter is open, and neutrons scattered from the ^{238}U target. The ambient neutron background is measured with no target present. The shape of the scatter background is estimated from a ^{208}Pb target. ^{208}Pb was chosen because it has a very small capture cross section, $\leqslant 0.1$ mb below 40 keV. Above 40 keV, there are capture resonances with cross sections approaching 1 b, but these can be eliminated by a gate on the summed-energy spectrum above the ^{208}Pb(n,γ) Q value of 3.94 MeV. The measured shape of the scatter background is normalized to the summed-energy spectrum from the target above the target capture Q value for each neutron energy bin, after ambient background subtraction as described below.

The relative contribution of these backgrounds to the $M_{cl} \geqslant 2$ summed-energy spectrum, for the 1 to 10 keV neutron energy range, is shown in Fig. 2. The ^{208}Pb spectrum is normalized to the ^{238}U spectrum in the 6 to 10 MeV region, the no-target spectrum was normalized by neutron monitor counts to the ^{238}U spectrum, and the no-beam spectrum was normalized by time to the ^{238}U spectrum.

The counts corresponding to neutron capture were corrected for backgrounds using the following formulas:

$$N = U_Q - n_{uo}O_Q - r_{\text{scat}}(Pb_Q - n_{po}O_Q), \tag{1}$$

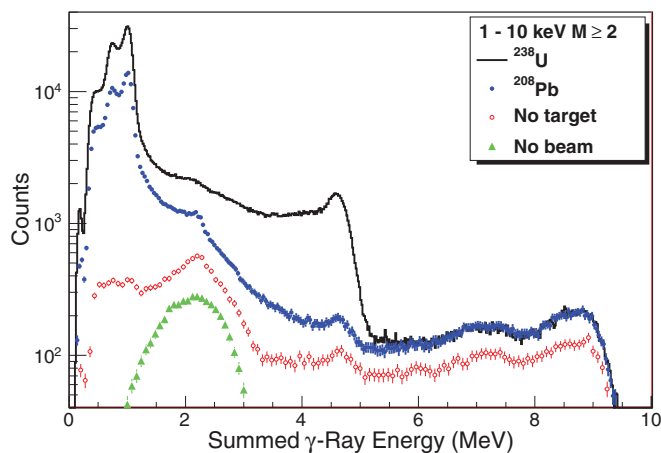$$r_{\text{scat}} = \frac{U_s - n_{uo}O_s}{Pb_s - n_{po}O_s}, \tag{2}$$

FIG. 2. (Color online) Summed gamma-ray energy spectra for reactions with neutron energies between 1 and 10 keV and gamma-ray multiplicity $M_{cl} \geqslant 2$.

where U_s and U_Q are the counts in the ^{238}U spectra subject to gates on summed energy for the scattering region and the region corresponding to the Q value of the capture reaction, respectively. O_Q and O_S are the counts in the no-target spectra, and Pb_S and Pb_Q are counts in the the ^{208}Pb spectra used to estimate the neutron-scattering contribution. n_{uo} and n_{po} are the ratios of neutron monitor counts for the ^{238}U and no-target runs, and the ^{208}Pb and no-target runs, respectively. The monitor counts were taken from hardware scalers counting the ^{6}Li$(n,$t$)$ monitor in the thermal energy region. The Q value for ^{238}U(n,γ) is 4.81 MeV, and all target counts were determined from spectra with cluster multiplicity $\geqslant 2$ and summed-energy gate = 4.25 to 5.25 MeV. The time-of-flight data were binned into spectra with $dE/E = 5\%$ bins for neutron energies above 10 keV, for $dE/E = 2\%$ bins for energies between 1 and 10 keV, and with $dE/E = 0.1\%$ bins in the resonance region.

C. Cross-section measurement

The ^{238}U(n,γ) cross section has been extensively studied in the resonance region, and in this work we normalize our measurement to resonance cross sections calculated using parameters from the ENDF/B-VII.1 evaluation [6]. The resonances are broadened by the moderator resolution function, so integrals over the resonance, which are invariant under broadening, were calculated. The effects of self-attenuation and multiple scattering must also be considered, and the resonance integrals were calculated using the infinite slab model implemented in the SAMMY code [7]. In addition, only the weak s-wave resonances at 80.75, 145.67, and 165.30 eV were used. For these resonances, the self-attenuation and multiple scattering corrections were less than 1%. The standard deviation of the three normalization factors was 1.3%, which is taken to be the normalization uncertainty in the cross section. The energy-dependent uncertainties were determined from the statistical uncertainties in capture counts and neutron flux.

The measured cross sections with this normalization are compared to the cross sections calculated from the ENDF/B-VII parameters in Fig. 3. The resonances were broadened using the "RPI" moderator function in the SAMMY code with parameters from Ref. [8].

D. Gamma-ray spectra

The individual gamma-ray spectra from the capture cascade provide an additional constraint on the level density and strength functions used in the calculation of the capture cross section. Gamma cascades were measured for selected $1/2^+$ resonances, and compared to spectra calculated using the DICEBOX code [9], as discussed in Sec. III.

The spectra were measured by gating on individual neutron resonances to maximize the signal-to-background ratio and using a gate of 4.2 to 5.5 MeV window on the summed-energy spectrum. After the data-reduction gates, the count rate from the blank target and the ^{208}Pb target were the same, indicating that in this energy region the target backing plus ambient background were the dominant background components. The $M_{cl} = 2$ data gated on the 36 eV resonance along with the blank background are shown in Fig 4. The background was
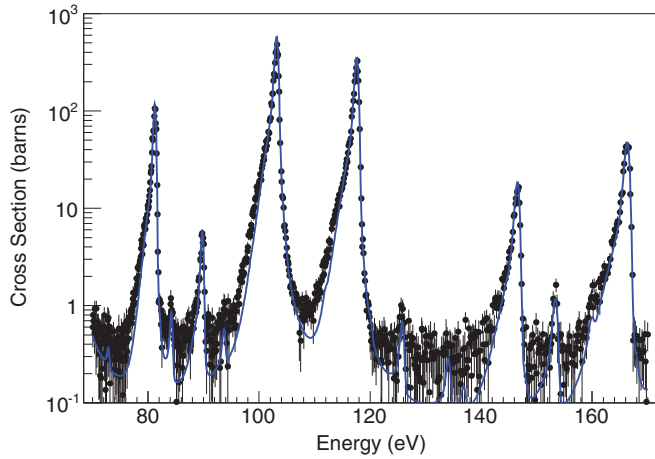
FIG. 3. (Color online) Normalized ^{238}U(n,γ) Measurement. The 80.75, 145.67, and 165.30 eV resonances were used for normalization. The cross section calculated using resonance parameters from ENDF/B-VII.1, broadened by the moderator function, is also shown. The data are binned in $dE/E = 0.1\%$ energy bins.

normalized to the ^{238}U by using the ^{235}U$(n,$f$)$ monitor. For these gates, the decay component was less than 10% of the blank background, and was neglected.

The measured spectra were not corrected for detector response, but are compared to calculated spectra propagated through a GEANT4 model of the DANCE array [10].

III. CALCULATIONS OF GAMMA-RAY SPECTRA

Additional information on the capture process can be obtained from the gamma-ray spectrum from cascades with different gamma multiplicity. Model calculations of the gamma-ray spectra were made with the code DICEBOX [9] which pays particular attention to the fluctuations inherent in the statistical model and includes explicit calculation of internal conversion. The fluctuations are obtained from the
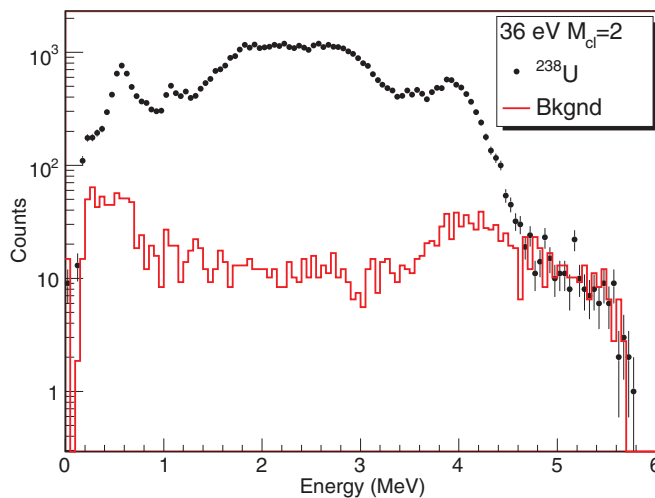
simulation of different "artificial nuclei" which are called "nuclear realizations." DICEBOX generates a Monte Carlo list of cascade gammas which were then processed through a well-tested GEANT4 model [10] of the DANCE array to account for the detector response. The processed events were analyzed with the same data reduction gates as the measured data, and the resulting multiplicity, gamma-ray energy spectrum, and total gamma energy spectrum were compared directly to the measurements.

DICEBOX uses the measured levels from the Evaluated Nuclear Structure Data File (ENSDF) [1] up to a critical energy of $E_{crit} = 0.847$ MeV, and levels generated from a level-density formula above that. A constant-temperature level density has been shown to be appropriate for the U isotopes [11] and the constant-temperature parametrization of von Egidy and Bucurescu with an energy-independent spin cutoff [12] was used in this work. For the $E1$ radiative strength function, we choose to use the generalized Lorentzian (GLO) form [13]. The giant dipole parameters for the GLO were taken from the systematic fits in RIPL-3 [14]. Models for the $E1$ strength function are all based on (γ,n) measurements, which have a threshold at the neutron separation energy, 4.81 MeV in ^{239}U. Different models extrapolate different behavior below the separation energy. This issue is discussed in some detail in Ref. [15]. In addition, a single-particle $E2$ contribution was also used, which had negligible impact on the results.

Twenty DICEBOX realizations were calculated. The average of the realizations is compared with the measured multiplicity 2 and 3 spectra in Figs. 5 and 6. The data are from four resonances at 21, 36, 66, and 102 eV. For comparison, the experimental data and calculations were all normalized to have the same area as the 36 eV resonance. The calculated spectra (GLO No $M1$) do not provide a good representation of the data.

In addition to the $E1$ giant dipole contribution to the radiative strength function, there are other well studied low-lying contributions of $E1$ and $M1$ strength. This strength includes the pygmy $E1$, the Gamow-Teller (spin-flip $M1$), and the $M1$ scissors mode giant resonances. The strength that is weighted
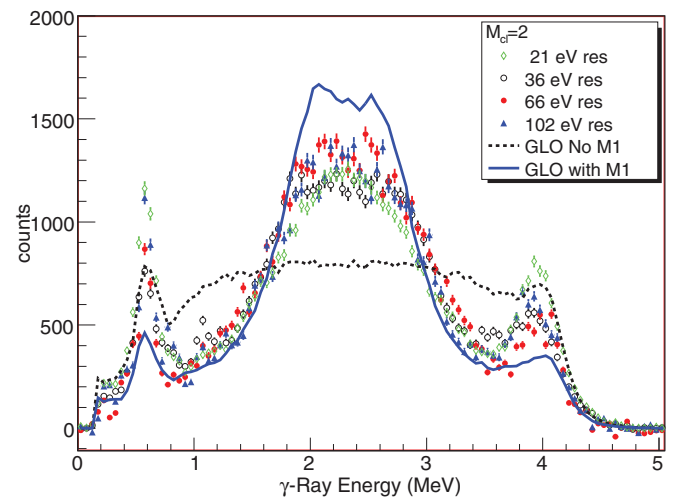

FIG. 4. (Color online) Spectrum of γ rays with $M_{cl} = 2$ from the decay of the 36 eV resonance in ^{238}U(n,γ) compared to the blank background subject to the same data reduction gates.

FIG. 5. (Color online) Spectrum of γ rays from the decay of the four resonances in ^{238}U(n,γ), $M_{cl} = 2$, compared with DICEBOX calculations (GLO) with parameters as described in the text.
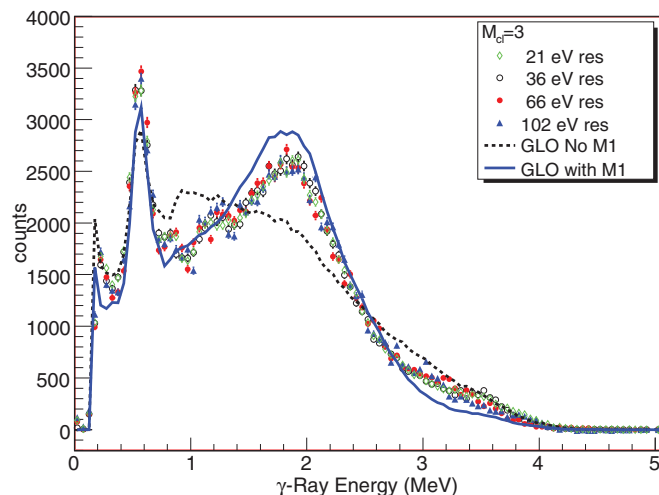
FIG. 6. (Color online) Spectrum of γ rays from the decay of resonances in ^{238}U(n,γ), $M_{cl} = 3$, compared DICEBOX calculations.

FIG. 7. (Color online) Comparison of DICEBOX prediction of gamma-ray spectrum for $M_{cl} = 2$ cascades in ^{238}U(n,γ), using the GLO model with no-scissors mode (blue) and the calculation including the scissors mode (red). The figure shows the range of $\pm 1\sigma$ for 20 realizations.

most strongly by the level density is the low-lying $M1$ scissors mode (SM) resonance [see Eq. (3)]. The SM resonance has been extensively studied by electron scattering and found to have an excitation centroid of approximately $66\delta A^{-1/3}$ MeV, where δ is the quadrupole deformation parameter [16]. This corresponds to an excitation energy of 2.24 MeV in ^{239}U.

Low-lying $M1$ "scissors-mode" strength has been observed and predicted in several even-even actinide nuclides. Experimentally, studies of scissors-mode excitation by nuclear resonance fluorescence in the actinides have been reported for ^{232}Th [17,18], ^{235}U [19], ^{236}U [20], and ^{238}U [18,21]. Theoretical studies using a sum rule approach [22] and using the random-phase approximation [23–25] on these nuclei have also been reported. The experimental and theoretical situation for ^{232}Th, ^{236}U, and ^{238}U has been carefully summarized by Hammond [21]. Studies of the scissors-mode resonance excited by d and ^{3}He reactions in ^{231,232,233}Th and ^{232,233}Pa using the "Oslo method" [26] have also been reported.

Calculations indicate that the centroid and integrated strength in odd nuclei should be very similar to the adjacent even nuclei [22,27] although there are indications it may be strongly fragmented and spread over a wider energy range [28]. A recent NRF measurement on ^{235}U at HiγS [19] with gamma rays from 1.6 to 3.0 MeV indicated that the centroid of the M1 strength is located at about 1.8 MeV, considerably lower than the predicted energy of about 2.8 MeV, and that the integrated strength was approximately 0.30 μ_N^2, considerably lower than the values of 4.0 to 8 μ_N^2 observed in ^{236,238}U.

It has been observed that the analysis of Ref. [28] does not always produce consistent results [29] and it is not clear that NRF measurements provide an adequate characterization of the scissors-mode strength inferred from (n,γ) reactions in odd-mass nuclei [15]. In the recent work by Kroll $et\ al.$ [15], it is observed that the radiative strength function inferred by the Oslo method for the Gd and Dy mass regions provides a good description of (n,γ) reactions on the Gd isotopes.

Although behavior in the rare earths may not be the same as in the actinides, we elected to try adding the $M1$

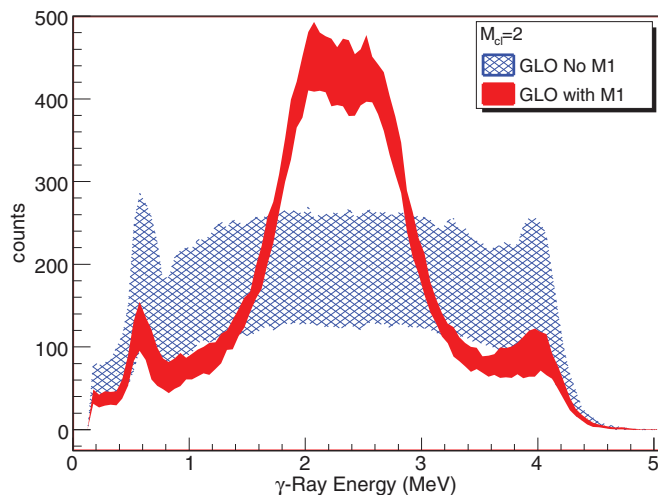scissors-mode strength obtained from the Oslo M ethod [26] in our DICEBOX calculations, using the standard Lorentzian parameters obtained for ^{233}Th with no $ad\ hoc$ renormalization. These calculations, normalized to the area of the 36 eV resonance, are also compared to the data in Figs. 5 and 6. A comparison of the $\pm$ one-standard-deviation range of the 20 realizations for the DICEBOX calculations with and without the $M1$ scissors mode is shown in Figs. 7 and 8.

Inclusion of the $M1$ scissors mode in the radiative strength function provides a qualitatively better representation of the shape of the gamma-ray spectra. It is likely that judicious "tuning" of the parameters could produce an even better description of the data. This is not conclusive identification
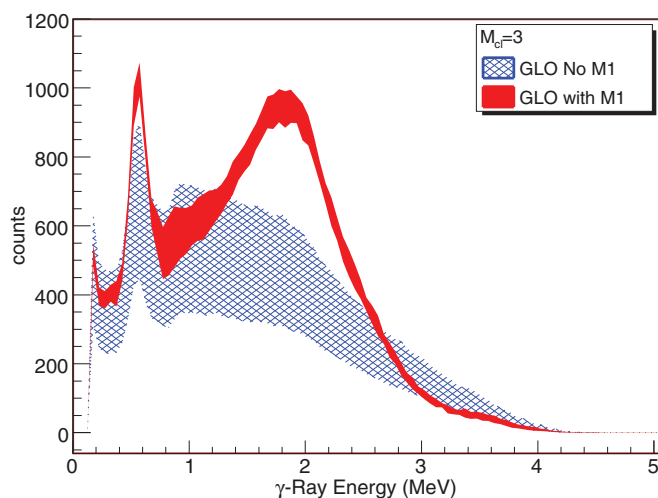

FIG. 8. (Color online) Comparison of DICEBOX prediction of gamma-ray spectrum for $M_{cl} = 3$ cascades in ^{238}U(n,γ), using the GLO model with no-scissors mode (blue) and the calculation including the scissors mode (red). The figure shows the range of $\pm 1\sigma$ for 20 realizations.
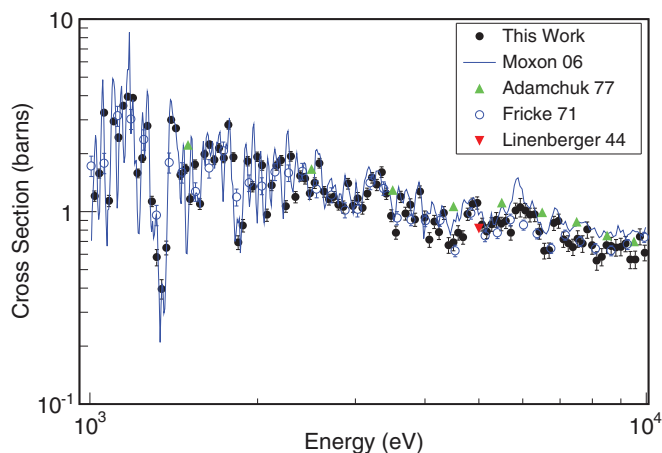
FIG. 9. (Color online) Measured $^{238}U(n,\gamma)$ cross section compared to previous measurements by Moxon [31], Adamchuk [32], Fricke [30] and Linenberger [33].

of $M1$ strength, but its presence is consistent with systematics and measurements in nearby nuclei. In general, any model combination which does not have a resonance-like behavior near $E_\gamma = 2.3$ MeV is unable to reproduce the bumps in the experimental spectra.

IV. CROSS-SECTION RESULTS

The data from this measurement from 1 to 10 keV, binned in $dE/E = 2\%$ energy bins, are shown in Fig. 9. Data from several previous measurements are also shown. The current data are in substantial agreement with Fricke [30], and differ slightly from the Moxon [31] measurements above about 3 keV. The very high quality Moxon data are shown as a continuous line, rather than individual points.

The data from this measurement above 10 keV, binned in $dE/E = 5\%$ bins, are compared to that from several previous measurements in Fig. 10. Data points from this
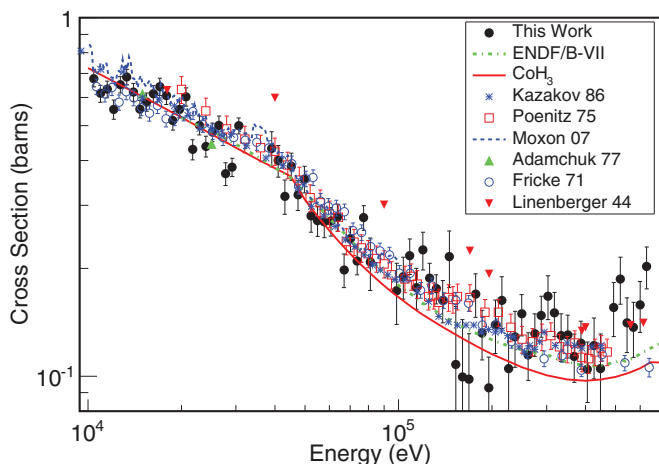

FIG. 10. (Color online) Measured $^{238}U(n,\gamma)$ cross section compared to previous measurements by Kazakov [34], Poenitz [35], Moxon [31], Adamchuk [32], Fricke [30], and Linenberger [33]. Also shown is the evaluated cross section from ENDF/B-VII.1 and the results of the model calculation (CoH$_3$) described in Sec. V.

work in the region of the strong Al resonances at 36, 88, and 104 keV were rejected because the difference in energy resolution in the monitors and the BaF$_2$ did not permit a good cross-section determination. Also shown is the ENDF/B-VII.1 evaluation [6].

V. STATISTICAL MODEL CALCULATION FOR ^{238}U NEUTRON CAPTURE

A. Model parameters

We performed statistical model calculations for the $^{238}U(n,\gamma)$ cross section above the resolved resonance region and compared with our measured data. Because the energy range of our interest is in the fast energy range, where the total excitation energy is lower than the fission barrier of ^{239}U, the most important competing channels are the neutron elastic and inelastic scattering, and radiative neutron capture reactions. We have paid a great deal of attention to the model parameters relevant to these reaction channels. The model calculation is performed with the CoH$_3$ statistical Hauser-Feshbach code [36].

CoH$_3$ combines the coupled-channels optical model and the statistical Hauser-Feshbach model calculations with the detailed balance method [37,38], where all the generalized transmission coefficients from the excited target are correctly calculated. To avoid a convergence problem in the coupled-channels method [39], six states (0^+, 2^+, 4^+, 6^+, 8^+, and 10^+) in the ground state rotational band are coupled. The width fluctuation correction is performed in the generalized transmission coefficient space to eliminate the direct reaction. Moldauer's width fluctuation model [40] is adopted with our updated systematics of the channel degree-of-freedom [41]. This new parametrization lowers the capture cross section slightly, by a few tenths of a percent.

We adopt the optical potential of Soukhovitskii *et al.* [42], with some adjustments to reproduce the evaluated neutron strength functions of $S_0 = 1.29 \times 10^{-4}$ and $S_1 = 2.17 \times 10^{-4}$ [43]. The Monte Carlo technique is adopted for the potential parameter search, where the six potential parameters (depth, radius, and diffuseness parameters for both real and imaginary potentials) are perturbed randomly within a few percent to seek for a set of parameters that match the evaluated $S_{0,1}$ values. Although the parameters obtained in such a way are not necessarily a unique solution, they are sufficient for our purpose. In fact the adjustment was rather modest, except for the diffuseness parameter of the real potential, which was reduced by 17%.

Since the neutron inelastic scattering channels are all in the discrete levels in our modeling, the continuum appears only in the γ-ray emission channel. The level densities in the continuum of ^{239}U are calculated with the composite level density formulas of Gilbert and Cameron [44] with an updated parametrization [45]. The level density parameter of ^{239}U is further tuned a little to reproduce the evaluated average s-wave resonance spacing D_0 of 20.3 eV. The parameter values used were $T = 0.4176$ MeV, $E_0 = -0.9185$ MeV, and $\sigma^2 = 8.88$. At low excitation energies of both ^{238}U and ^{239}U, the discrete level data are taken from the evaluated nuclear structure data base RIPL-3 [14] (updated in 2012).

The γ-ray transmission coefficient is calculated from the γ-ray strength functions. For the double-humped $E1$ strength we adopt the generalized Lorentzian form (GLO) of Kopecky and Uhl [13]. In addition to the higher multipolarities in the standard Lorentzian form taken from the parameter systematics in RIPL-3, we consider the $M1$ scissors mode as discussed in Sec. III.

B. Renormalization of γ-ray strength function

It is commonly understood that the neutron radiative capture cross section is very difficult to predict without any experimental information. This is partly due to the uncertainty in the adopted γ-ray strength function, where the simple Lorentzian shape is doubtless crude. To have consistent average properties of calculations in the resolved resonance region, the γ-ray strength function is often renormalized as

$$\frac{\langle \Gamma_\gamma \rangle}{D_0} = N \int_0^{S_n} \sum_{XL} E_\gamma^{2L+1} f_{XL}(E_\gamma) \rho(S_n - E_\gamma) dE_\gamma, \quad (3)$$

where $\langle \Gamma_\gamma \rangle$ is the average γ-ray width, S_n is the neutron separation energy, E_γ is the emitting γ-ray energy, $\rho(E_x)$ is the level density at the excitation energy of $E_x = S_n - E_\gamma$, and f_{XL} is the γ-ray strength function for the multipolarity of XL. When experimental $\langle \Gamma_\gamma \rangle$ and D_0 are given, the normalization constant N is calculated from Eq. (3).

Ideally this normalization factor would be near unity. However, it often deviates from unity nucleus by nucleus. For example, if we include only default γ-ray strength functions in CoH$_3$, and normalize them to $\langle \Gamma_\gamma \rangle/D_0 = 0.00115$ [43], the normalization constant is 2.4. This implies the calculated capture cross section is significantly lower than the average cross sections in the resonance region. When we add the scissors mode as discussed in Sec. III, the factor becomes $N = 1.1$. However, despite the large difference in the normalization factors in these cases, the calculated capture cross sections become almost identical when the strength functions are normalized in this manner. This conceals information regarding the γ-ray strength function in the statistical model calculations.

C. Comparisons with experimental data

The calculated capture cross sections are compared with the DANCE data, together with the evaluated cross section in ENDF/B-VII.1 [6]. in Fig. 11. The dotted line is the calculated result with the $M1$ scissors mode, while the dash-dotted line is the case when it is omitted. The strength function was not renormalized to $\langle \Gamma_\gamma \rangle/D_0$ ($N = 1.0$). The solid line is the evaluated cross section from ENDF/B-VII.1, which is based on the IAEA Standards evaluation [4] smoothed by the statistical model calculations. Without $M1$ or the normalization factor, the predicted capture cross sections are largely underestimated, as we recall we needed the normalization factor of 2.4. Inclusion of the $M1$ strength significantly improves the reproduction of evaluated data as well as the DANCE data. We emphasize that we had no intention to tune any model parameters to obtain this excellent agreement.
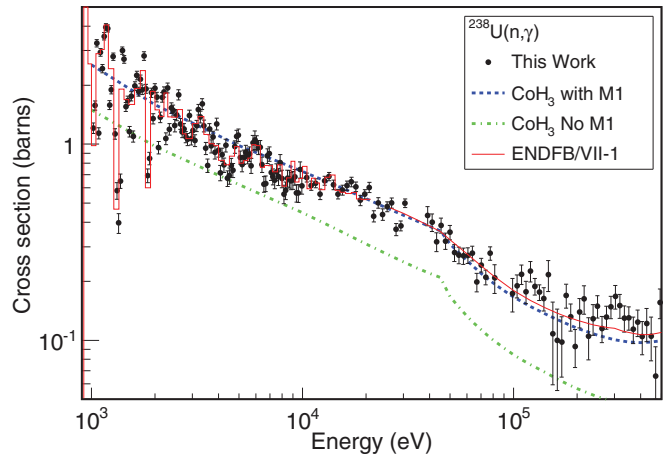

FIG. 11. (Color online) Comparison of calculated ^{238}U capture cross section with the DANCE data, as well as evaluated cross section in ENDF/B-VII.1. Below 20 keV the cross sections in ENDF, which are represented by the resonance parameters, are shown by the average in 640 energy groups.

Using Eq. (3) and renormalizing the calculated capture cross section to the evaluated data, we can estimate the average γ-ray width $\langle \Gamma_\gamma \rangle$. When we assume our calculated capture cross section at 50 keV to be 325 mb (note that JENDL-4 [46] has very similar value of 324 mb), $\langle \Gamma_\gamma \rangle$ could be 20 meV, and this is smaller than the compiled value of 23.36 $\pm$0.31 meV [43]. This inconsistency is also reported elsewhere [47].

VI. CONCLUSIONS

Measurements of the ^{238}U(n,γ) cross section from 1 to 500 keV, using the DANCE detector, confirm earlier measurements. Gamma-ray emission spectra provide an additional constraint on the calculations, and an $M1$ "scissors mode" contribution to the radiative strength function provided a good representation of the measured spectra. Hauser-Feshbach calculations of the capture cross section that do not rely on normalization to a measured $\langle \Gamma_\gamma \rangle$ were made using a radiative strength function that included the scissors mode contribution. These calculations provided a very good representation of the measured data. Similar calculations for nuclei for which $\langle \Gamma_\gamma \rangle$ is not known may be possible.

[1] www.nndc.bnl.gov.

[2] T. Kawano, N. Fujikawa, K. Yoshida, and Y. Kanda, in *Proceedings of the International Conference on Nuclear Data for Science and Technology (Gatlinburg)*, edited by J. K. Dickens (American Nuclear Society, La Grange Park, IL, 1994), p. 652.

[3] Y. Kanda and M. Baba, NEA Technical Report No. WPEC/SG4, Paris, 1999 (unpublished); Y. Kanda, Y. Kikuchi, Y. Nakajima, M. G. Sowerby, M. C. Moxon, F. H. Frohner, W. P. Poenitz, and L. W. Weston, in *Nuclear Data for Science and Technology*, edited by S. M. Qaim (Springer-Verlag, Berlin, 1992), p. 851.

[4] A. D. Carlson *et al.*, Nucl. Data Sheets **110**, 3215 (2009).

[5] M. Jandel *et al.*, Nucl. Instrum. Methods B **261**, 1117 (2007).

[6] M. B. Chadwick *et al.*, Nucl. Data Sheets **112**, 2887 (2011).

[7] N. M. Larson, Oak Ridge National Laboratory Report No. ORNL/TM-9179/R7, 2006 (unpublished).

[8] P. E. Koehler (private communication).

[9] F. Becvar, Nucl. Instrum. Methods A **417**, 434 (1998).

[10] M. Jandel *et al.*, Nucl. Instrum. Methods B **261**, 1117 (2007).

[11] M. Guttormsen *et al.*, Phys. Rev. C **88**, 024307 (2013).

[12] T. von Egidy and D. Bucurescu, Phys. Rev. C **72**, 044311 (2005).

[13] J. Kopecky and M. Uhl, Phys. Rev. C **41**, 1941 (1990).

[14] R. Capote *et al.*, Nucl. Data Sheets **110**, 3107 (2009); *Handbook for Calculations of Nuclear Reaction Data, RIPL-2, Reference Input Parameter Library*, IAEA-TECDOC-1506 (International Atomic Energy Agency, Vienna, 2006).

[15] J. Kroll *et al.*, Phys. Rev. C **88**, 034317 (2013).

[16] K. Heyde, P. von Neumann-Cosel, and A. Richter, Rev. Mod. Phys. **82**, 2365 (2010).

[17] A. S. Adekola, C. T. Angell, S. L. Hammond, A. Hill, C. R. Howell, H. J. Karwowski, J. H. Kelley, and E. Kwan, Phys. Rev. C **83**, 034615 (2011).

[18] R. D. Heil, H. H. Pitz, U. E. P. Berg, U. Kneissl, K. D. Hummel, G. Kilgus, D. Bohle, A. Richter, C. Wesselborg, and P. von Brentano, Nucl. Phys. A **476**, 39 (1988).

[19] E. Kwan, G. Rusev, A. S. Adekola, F. Donau, S. L. Hammond, C. R. Howell, H. J. Karwowski, J. H. Kelley, R. S. Pedroni, R. Raut, A. P. Tonchev, and W. Tornow, Phys. Rev. C **83**, 041601(R) (2011).

[20] J. Margraf, A. Degener, H. Freidrichs, R. D. Heil, A. Jung, U. Kneissl, S. Lindenstruth, H. H. Pitz, H. Schacht, U. Seemann, R. Stock, C. Wesselborg, P. von Brentano, and A. Zilges, Phys. Rev. C **42**, 771 (1990).

[21] S. L. Hammond, A. S. Adekola, C. T. Angell, H. J. Karwowski, E. Kwan, G. Rusev, A. P. Tonchev, W. Tornow, C. R. Howell, and J. H. Kelley, Phys. Rev. C **85**, 044302 (2012).

[22] J. Enders, P. von Neumann-Cosel, C. Rangacharyulu, and A. Richter, Phys. Rev. C **71**, 014306 (2005).

[23] A. A. Kuliev, E. Guliyev, F. Ertugral, and S. Özkan, Eur. Phys. J. A **43**, 313 (2010).

[24] V. G. Soloviev, A. V. Sushkov, N. Yu. Shirikova, and N. Lo Iudice, J. Phys. G: Nucl. Part. Phys. **25**, 1023 (1999).

[25] R. Nojarov, A. Faessler, P. Sarriguren, E. Moya de Guerra, and M. Grigorescu, Nucl. Phys. A **563**, 349 (1993).

[26] M. Guttormsen, L. A. Bernstein, A. Bürger, A. Görgen, F. Gunsing, T. W. Hagen, A. C. Larsen, T. Renstrøm, S. Siem, M. Weideking, and J. N. Wilson, Phys. Rev. Lett. **109**, 162503 (2012).

[27] J. N. Ginocchio and A. Leviatan, Phys. Rev. Lett. **79**, 813 (1997).

[28] J. Enders, N. Huxel, P. von Neumann-Cosel, and A. Richter, Phys. Rev. Lett **79**, 2010 (1997).

[29] A. Nord *et al.*, Phys. Rev. C **67**, 034307 (2003).

[30] M. P. Fricke, W. M. Lopez, S. J. Friesenhahn, A. D. Carlson, and D. G. Costello, Nucl. Phys. A **146**, 337 (1970). (Data points obtained from the CSISRS database [1].)

[31] M. C. Moxon (unpublished). (Data obtained through the CSISRS database[1]).

[32] Jy. V. Adamchuk, M. A. Voskanjan, G. U. Muradjan, G. I. Ustrojev, and Ju. G. Shchepkin, Proceedings of the All Union Conference on Nuclear Physics, Kiev, 1977, Vol. 2 (unpublished). (Data obtained through the CSISRS database [1].)

[33] G. A. Linenberger, J. Miskel, E. Segre, C. Bailey, J. Blair, D. Frisch, D. Greene, K. Greisen, A. O. Hanson, and J. Hush *et al.*, Los Alamos Scientific Laboratory Report No. 179, 1944 (unpublished.) (Data points obtained from the CSISRS database [1].)

[34] L. E. Kazakov, V. N. Kononov, G. N. Manturov, E. D. Poletaev, M. V. Bokhovko, V. M. Yimokhov, and A. A. Voevodskij, Vop. At. Nauki i Tekhn, Ser. Yadernye Konstanty **3**, 37 (1986). (Data points obtained from the CSISRS database [1].)

[35] W. P. Poenitz, Nucl. Sci. Eng. **57**, 300 (1975). (Data points obtained through the CSISRS database [1].)

[36] T. Kawano, P. Talou, M. B. Chadwick, and T. Watanabe, J. Nucl. Sci. Technol. **47**, 462 (2010)

[37] T. Tamura, Rev. Mod. Phys. **37**, 679 (1965).

[38] T. Kawano, P. Talou, J. E. Lynn, and M. B. Chadwick, and D. G. Madland, Phys. Rev. C **80**, 024611 (2009).

[39] F. S. Dietrich and I. J. Thompson, and T. Kawano, Phys. Rev. C **85**, 044611 (2012).

[40] P. A. Moldauer, Nucl. Phys. A **344**, 185 (1980).

[41] T. Kawano and P. Talou, in *Proceedings of the International Conference on Nuclear Data for Science and Technology* [Nuclear Data Sheets (to be published)].

[42] E. S. Chiba, J. Y. Lee, O. Iwamoto, and T. Fukahori, J. Nucl. Phys. G **30**, 905 (2004).

[43] S. F. Mughabghab, *Atlas of Neutron Resonances, Resonance Parameters and Thermal Cross Sections, Z = 1–100* (Elsevier, Amsterdam, 2006).

[44] A. Gilbert and A. G. W. Cameron, Can. J. Phys. **43**, 1446 (1965).

[45] T. Kawano, S. Chiba, and H. Koura, J. Nucl. Sci. Technol. **43**, 1 (2006); T. Kawano (unpublished).

[46] K. Shibata *et al.*, J. Nucl. Sci. Technol. **48**, 1 (2011).

[47] A. Plompen, T. Kawano, and R. Capote Noy, IAEA Report No. INDC(NDS)-0597, 2012 (unpublished).